AGU PUBLICATIONS

Geophysical Research Letters

RESEARCH LETTER
10.1002/2015GL064007

Key Points:
- Ganglion dynamics contributes to nonwetting phase transport
- Coalescence of nonwetting phase clusters is triggered by snap off
- Ganglion dynamics occurs from 75% nonwetting phase saturation on

Supporting Information:
- Text S1 and Figures S1–S7

Correspondence to:
S. Berg,
steffen.berg@shell.com

Citation:
Rücker, M., et al. (2015), From connected pathway flow to ganglion dynamics, *Geophys. Res. Lett.*, *42*, 3888–3894, doi:10.1002/2015GL064007.

Received 27 MAR 2015
Accepted 22 APR 2015
Accepted article online 20 MAY 2015
Published online 23 MAY 2015

From connected pathway flow to ganglion dynamics

M. Rücker[1,2], S. Berg[1], R. T. Armstrong[3], A. Georgiadis[1], H. Ott[1], A. Schwing[1], R. Neiteler[1], N. Brussee[1], A. Makurat[1], L. Leu[1,2], M. Wolf[2], F. Khan[2], F. Enzmann[2], and M. Kersten[2]

[1]Shell Global Solutions International B.V., Rijswijk, Netherlands, [2]Geosciences Institute, Johannes Gutenberg University, Mainz, Germany, [3]School of Petroleum Engineering, University of New South Wales, Sydney, New South Wales, Australia

Abstract During imbibition, initially connected oil is displaced until it is trapped as immobile clusters. While initial and final states have been well described before, here we image the dynamic transient process in a sandstone rock using fast synchrotron-based X-ray computed microtomography. Wetting film swelling and subsequent snap off, at unusually high saturation, decreases nonwetting phase connectivity, which leads to nonwetting phase fragmentation into mobile ganglia, i.e., ganglion dynamics regime. We find that in addition to pressure-driven connected pathway flow, mass transfer in the oil phase also occurs by a sequence of correlated breakup and coalescence processes. For example, meniscus oscillations caused by snap-off events trigger coalescence of adjacent clusters. The ganglion dynamics occurs at the length scale of oil clusters and thus represents an intermediate flow regime between pore and Darcy scale that is so far dismissed in most upscaling attempts.

1. Introduction

Multiphase flow in porous media is constituted by the interplay of viscous and capillary forces. Capillarity leads to a rich set of phenomena that are ultimately manifested as the commonly observed hysteresis and irreducible residual saturations of wetting (w) and nonwetting (nw) phases. Capillarity is also what limits the recovery of nonwetting phase during enhanced oil recovery operations [*Lake*, 1989]. On the Darcy scale, residual saturations are embedded into the relative permeability and capillary-pressure-saturation relationships. However, these parameters must be determined independently, i.e., the classical two-phase Darcy formalism does not allow for the prediction of residual saturations. A generalized theory for two-phase flow in porous media which combines connected and disconnected phases leading to hysteresis and entrapment has been developed by Hilfer and coauthors [*Hilfer*, 2006a, 2006b; *Doster and Hilfer*, 2011], where the basic idea was already formulated in *Hilfer* [1998]. Over several decades ago, the pore-scale mechanisms of snap off [*Roof*, 1970] and corner flow [*Mohanty et al.,* 1987] were established to be responsible for the disconnection and thus trapping of nw phase. While we have a good view on the initial and final states of this process [*Andrew et al.,* 2013; *Murison et al.,* 2014; *Iglauer et al.,* 2011; *Pak et al.,* 2015; *Chaudhary et al.,* 2013; *Deng et al.*, 2014], it is far less clear how we actually arrive from an initially connected pathway flow to trapped nw phase [*Datta et al.,* 2014; *Krummel et al.,* 2013; *Lenormand et al.,* 1983].

Such a transition occurs, for example, during an oil recovery water flood, when an initially high oil saturation, which is presumably connected, is ultimately reduced to trapped disconnected immobile oil. To a large extent, the transition occurs in the capillary dispersion zone at the shock front of the displacement [*Buckley and Leverett*, 1942; *Lake*, 1989], as sketched in Figure 1. However, the macroscopic saturation profiles that are well described by the two-phase extension of Darcy's law offer only very little insight as to what the associated flow regimes are at the pore scale, where capillary forces play a dominating role. The difficulty in establishing a consistent understanding of pore-scale displacement is evident from the paradox [*Cense and Berg*, 2009] that in the extended two-phase Darcy formalism, on sufficiently large length scales, flow is viscous dominated (and the two-phase extension of Darcy's law is formulated in a viscous structure while capillary effects are lumped into relative permeability), whereas two-phase flow is capillary dominated at the pore scale (where capillary forces dominate over gravity) [*Hilfer and Øren*, 1996].

Ganglion dynamics [*Avraam and Payatakes*, 1995; *Hilfer*, 2006a, 2006b] offers a way of resolving the paradox. The pore-scale process is capillary dominated but the collective transport, when averaged, starts to behave as if viscous dominated. The experimental work by Avraam and Payatakes [*Avraam and Payatakes*, 1995] conducted on 2-D micromodels demonstrates that at the pore scale, connected pathway flow and ganglion

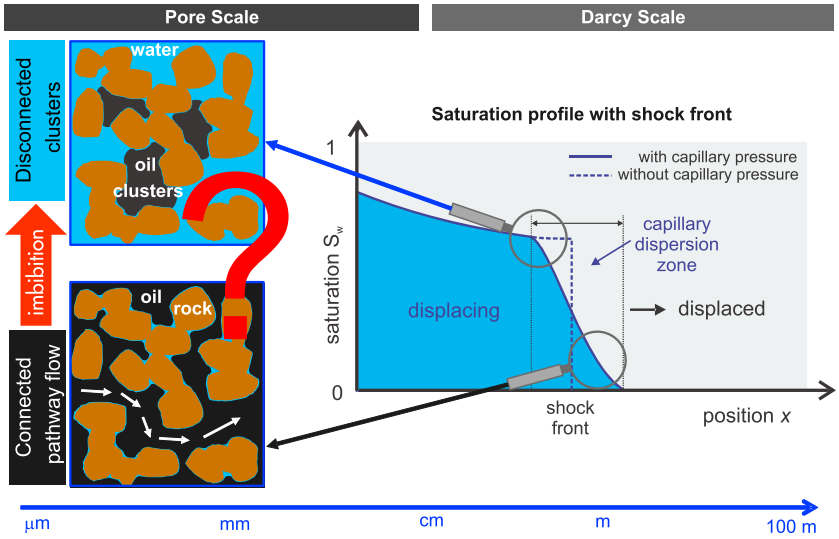

Figure 1. On the Darcy scale, imbibition is associated with a distinct saturation profile with a shock front, which under the influence of capillarity is broadened into a capillary dispersion zone. It is far less clear how on the pore scale, within the capillary dispersion zone, the flow regimes change from connected pathway flow of the initially connected oil to disconnected, resulting in trapped oil. Synchrotron-based fast X-ray computed microtomography allows us to follow the transient process step by step.

dynamics occur side by side. The oil clusters [*Andrew et al.,* 2013] that span over several individual pores flow through a sequence of breakup and coalescence processes, which contributes to mass transfer. In the generalized theory for two-phase flow in porous media by Hilfer, breakup and coalescence are the processes responsible for the exchange between connected and disconnected phases [*Doster and Hilfer*, 2011].

However, it is unclear how the 2-D results of Payatakes and Avraam translate to a 3-D porous medium where several relevant conditions like percolation thresholds and long-range connectivity of the wetting phase through corner flow [*Mohanty et al.,* 1987] are different. It is also unclear which saturation ranges the different flow regimes correspond to. Which saturation marks the transition from connected pathway flow to ganglion dynamics, over what saturation range does ganglion dynamics occurs, and at what saturations are oil clusters immobile?

Here we present a study where the pore-scale displacement of oil and brine is imaged during imbibition in a sandstone rock by using synchrotron-based fast X-ray computed microtomography (μCT) [*Berg et al.,* 2013; *Youssef et al.,* 2014]. We find that the onset of ganglion dynamics occurs at high oil saturations (around 75%), which is preceded by a regime of corner flow and film swelling that decreases the connectivity of the nonwetting phase. In the ganglion dynamics regime, oil clusters are not yet capillary trapped but remain mobile over a wide saturation range until they start becoming immobile around an oil saturation of 30%. Ganglion dynamics coexists with connected pathway flow and contributes to the transport of oil. The contribution of connected pathway flow decreases as the cluster, which percolates between the inlet and outlet, fragments into smaller disconnected ganglia.

Through direct imaging, we gain novel details about the ganglion dynamics flow regime. Ganglion dynamics occurs in a capillary-dominated flow regime where oil clusters are not mobilized by viscous forces but by a sequence of breakup and coalescence processes that are driven by capillary pressure differences over single clusters. One of the key findings is that coalescence appears to be triggered by meniscus oscillations caused by large snap-off processes. Similar to drainage, also in imbibition, nonlocal effects and cooperative displacement are key to understanding the pore-scale flow characteristics. The local displacement is generally much faster than the average and/or externally applied flow suggests, which results in large local viscous forces and potential contributions of inertial forces.

2. Methods

The 3-D images were obtained by using synchrotron-based X-ray computed microtomography at the TOMCAT beamline (Paul Scherrer Institute, Swiss Light Source). The spatial resolution was of 2.2 μm (voxel length) and

the time resolution was of 40 s. The flow cell was designed specifically for fast μCT, with a built-in micropump for pulse-free continuous injection at low flow rates [*Berg et al.,* 2013]. A cylindrical sample (diameter = 4 mm, length = 10 mm) of Gildehauser sandstone (Bentheimer formation, μCT scan, and pore size distribution are shown in Figure S1 in the supporting information, with porosity $\varphi = 20\%$, permeability $K = 1.5 \pm 0.3$ D) was used for imbibition experiments with an injection rate = 0.1 μL/min, which corresponds to a capillary number of $Ca_{micro} = \mu_w \cdot v/\sigma = 1.8 \cdot 10^{-8}$ (with the water viscosity μ_w, water interstitial flow velocity v, and water-oil interfacial tension σ). For fluids, we used n-decane as nonwetting phase and water, doped with CsCl at a 1:6 weight ratio to increase the X-ray contrast, as the wetting phase. The interfacial tension σ between both fluids was 30 mN/m. Before the imbibition experiment started, the sample was first saturated with the CsCl brine, which was then displaced by oil (primary drainage), arriving at an initial oil saturation of 78% while the water phase remained connected over the whole sample (see Figure S2). Image processing was performed with Avizo Fire 8.1 (FEI) and involved filtering (nonlocal means) and watershed segmentation obtaining the nonwetting and wetting phase distribution (see the supporting information for details).

From the time series of segmented images not only was saturation determined but also the Euler characteristic χ which is a measure for the topology of an object and used in this work to determine through how many individual pore throats the nonwetting phase clusters are internally connected. In the context of the nonwetting phase in porous media, the Euler characteristic χ can be decomposed into the number of objects (β_0, the zeroth Betti number, here the number of clusters) minus the number of redundant loops (β_1, the first Betti number), $\chi = \beta_0 - \beta_1$ [*Herring et al.,* 2013, 2015; *Schlüter et al.,* 2014] (for more details, see Figure S6 where we show β_0, β_1, and $\chi = \beta_0 - \beta_1$ as a function of time). From the time series, also displacement events (snap off and coalescence) [see also *Berg et al.,* 2015] were determined by subtracting fluid distributions of consecutive time steps (for more details see Figure S3), which also allowed statistics to be obtained on the displacement events. The connected single-phase permeability was computed with a direct Navier-Stokes-Brinkman solver using the commercial GeoDICT code (Math2Market, Kaiserslautern, Germany). The relative permeability for the connected oil phase is the (connected phase) oil permeability divided over the absolute permeability of the porous media saturated 100% with water phase.

3. Results and Discussion

The results displayed in Figure 2 suggest that imbibition occurs in two distinct regimes, where in the first "regime 1" the oil saturation decreases only very little and the oil phase mainly stays connected (Figure 2a, red); followed by "regime 2", where the oil phase breaks up into individual clusters (Figure 2a, yellow) accompanied by a substantial decrease in oil saturation from 75% to 30% (Figure 2b). The onset of cluster breakup, which occurs at an oil saturation of approximately 75% (consistent with *Joekar-Niasar et al.* [2013]), is marked by a sharp increase in the snap-off events (Figure 2d).

In regime 1, there is one dominating oil cluster, which initially contains 99% of the total oil volume and is connected across the whole sample, providing a connected pathway for the flow of oil. While in regime 1, the saturation changes only very little, the Euler characteristic $\chi = \beta_0 - \beta_1$ of the oil phase increases. That indicates a decrease in connectivity within the connected oil phase, which finally leads to breakup into isolated, nonpercolating clusters. If the rock was saturated 100% by oil, β_1 is negative due to the loops through pore bodies and pore throats leading to high connectivity. While in regime 1, the oil stays connected, i.e., $\beta_0 = 1$ for the biggest cluster that contains 99% of the total oil, β_1 decreases. That is caused by "loops" (i.e., internal connectivity in the oil cluster through multiple pores and pore throats) being removed through snap-off processes (Figure 2d) disconnecting oil in pore throats, and hence χ increases as displayed in Figure 2e. This causes also a slight decrease in the connected oil phase relative permeability as shown in Figure 2c. Therefore, regime 1 is mainly characterized by wetting film swelling and reduction of the nonwetting oil phase connectivity through redundant loops that have little effect on phase permeability.

In regime 2, we observe a transition from a connected oil phase flow (Figure 2a, red) to disconnected clusters (Figure 2a, yellow), which break off from the connected oil phase as fragments of increasing size. [*Berg et al.,* 2015] provide for a more detailed view how clusters break up and what the impact on the cluster size distribution is. In this process, the fraction of connected oil phase decreases and the number of clusters β_0

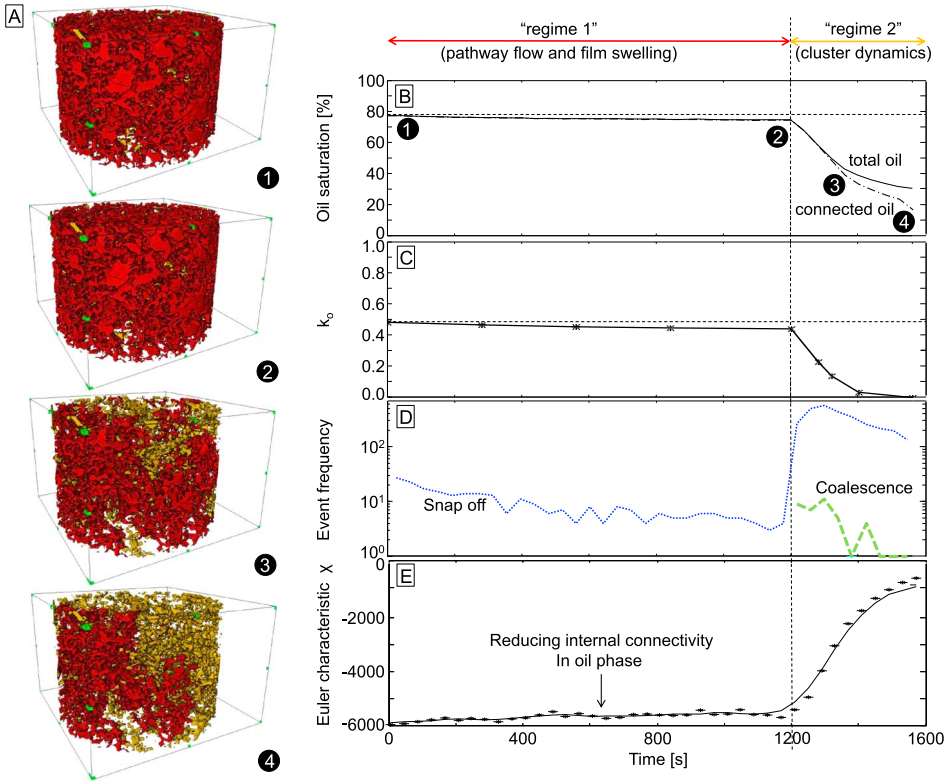

Figure 2. (a) During the imbibition experiment in the Gildehauser sandstone, the initially connected oil (red) breaks up into disconnected clusters (yellow). (b) Imbibition occurs in two distinct phases where first the saturation decreases only very little and the oil stays connected, corresponding to the swelling of the wetting phase film(s) (regime 1). Breakup events cause a strong decrease in oil saturation from 75% to 30% (regime 2). The fraction of connected oil decreases, and oil becomes increasingly disconnected. (c) The relative permeability of the connected oil phase follows the saturation trend decreasing only slightly in regime 1 but shows a rapid decrease in regime 2 as connected oil phase saturation substantially decreases. During the film-swelling phase, only snap-off events are observed. (d) In cluster dynamics regime 2, the frequency of the snap-off events increases and also oil coalescence events occur. (e) The Euler characteristic of the oil phase indicates that during the film-swelling phase, the internal connectivity of the percolating oil phase decreases until it reaches local percolation thresholds and breaks up into individual clusters.

increases. At the same time, the connectivity β_1 further decreases, which leads to a strong increase in χ as displayed in Figure 2e; and consequently, the relative permeability of the connected oil phase decreases (Figure 2c).

In regime 2, there is coexistence between two flow regimes: (1) connected pathway flow and (2) ganglion dynamics. When the fraction of connected oil saturation decreases, the associated (connected pathway) relative permeability decreases to values $<$0.04. However, the total oil saturation keeps decreasing by another 10%, and snap-off and coalescence events still frequently occur. This indicates that oil transport may not only occur through connected pathway flow but also through mobile clusters (but at this moment in time, we can unfortunately not quantify the exact contributions). This can also be seen from the fact that not only the biggest cluster decreases over time but also the fragments become in most cases smaller [*Berg et al.*, 2015], while the overall oil saturation decreases, i.e., fragments breaking up into smaller pieces do not explain the decrease in oil saturation. This is already an important observation in itself because it clearly shows that clusters remain mobile even though the flow regime is characterized as capillary dominated. For the length scale and flow rate investigated in this experiment, viscous forces exerted by the wetting phase flow are not sufficient to mobilize nonwetting phase clusters. In order to mobilize an oil cluster, the viscous pressure drop over the cluster (caused by the average flow field v) has to overcome the capillary forces associated with a narrow pore throat which is the case for faster flow rates and could also be the case for longer samples (not accessible to the μCT field of view associated with

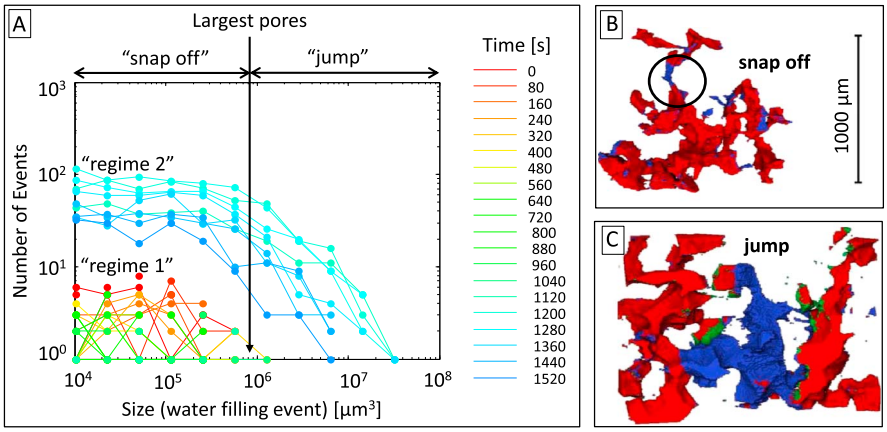

Figure 3. (a) The event statistics show that in the cluster break phase the snap-off events increase both in frequency and in magnitude (events extend over multiple pores) by up to 2 orders of magnitude. Intrapore events occurring in pore throats are called (b) snap off, while interpore events larger than a pore correspond to (c) Haines jumps [*Berg et al.,* 2013].

pore-scale resolution). The capillary number Ca^{macro} describing this balance [*Armstrong et al.,* 2014] is here approximated as

$$Ca^{\text{macro}} = \frac{l^{\text{cl}}}{r_{\text{p}}}\varphi\frac{\mu_w v}{\sigma} \tag{1}$$

where l^{cl} is the average cluster length, and r_{p} the radius of a pore throat. Ca^{macro} values range between 9.1×10^{-7} and 1.3×10^{-6}, which are several orders of magnitude smaller than unity. Therefore, on the basis of the average flow field, the flow regime was capillary dominated and one would not expect cluster mobilization by viscous forces.

In the capillary-dominated flow regime, clusters rather remain mobile through a sequence of breakup and coalescence processes evident from the event statistics in Figure 2d and also occur homogeneously over the whole sample length (see Figure S4). While breakup through snap off is an expected phenomenon in imbibition [*Roof*, 1970], it is much less clear what causes coalescence. The event statistics shown in Figure 2d provide a first clue because the onset of coalescence events coincides with the sharp increase in snap-off events. A more detailed analysis of the event statistics displayed in Figure 3a reveals that at the onset of regime 2 not only the frequency of the snap-off events increasing but also the associated displaced volume. Besides the more classical snap off in a single pore throat (Figure 3b) [*Roof*, 1970; *Deng et al.,* 2014], we observe much larger "jump" events that exceed the size of several pores (Figure 3c) and are not accounted for in common percolation models [*Dias and Wilkinson*, 1986].

The observation of coincidence between coalescence and the increase in frequency and magnitude of snap off alone does not provide a proof of causality. Observations in 2-D micromodels recorded with a high-speed camera at millisecond time resolution, which captures the interfacial dynamics during pore-scale events, show that snap off in one pore can trigger meniscus oscillations within the same cluster at a distant pore (for detailed image sequence of meniscus oscillations during snap off, see Figure S5). Similar observations of such nonlocal dynamics have already been observed during drainage [*Armstrong et al.,* 2014; *Andrew et al.,* 2014]. Even though the average flow velocity is low and hence the capillary number (equation (1)) indicates capillary-dominated flow, phase velocities associated with individual pore-scale events are generally high [*Quéré and Raphaël*, 1999; *Ferrari and Lunati*, 2014; *Armstrong and Berg*, 2013; *Moebius and Or,* 2014b]. The associated high-phase velocities extend over several pores [*Armstrong et al.,* 2015], approach Reynolds numbers of 1 [Armstrong, 2015], and meniscus oscillations are observed [*Quéré and Raphaël*, 1999; *Moebius and Or*, 2014a; *Ferrari and Lunati*, 2014], which indicates that inertial forces need to be considered [*Quéré*, 1997; *Ferrari and Lunati*, 2014; *Moebius and Or*, 2014a]. During imbibition when an interfacial jump occurs, local high velocities can extend over multiple pores, as explained in more detail in *Armstrong et al.* [2015]. The oil that redistributes after such an event may be influenced by the local velocity field and thus cause coalescence between clusters that are separated by perhaps one pore throat or within the "zone of influence" of the event.

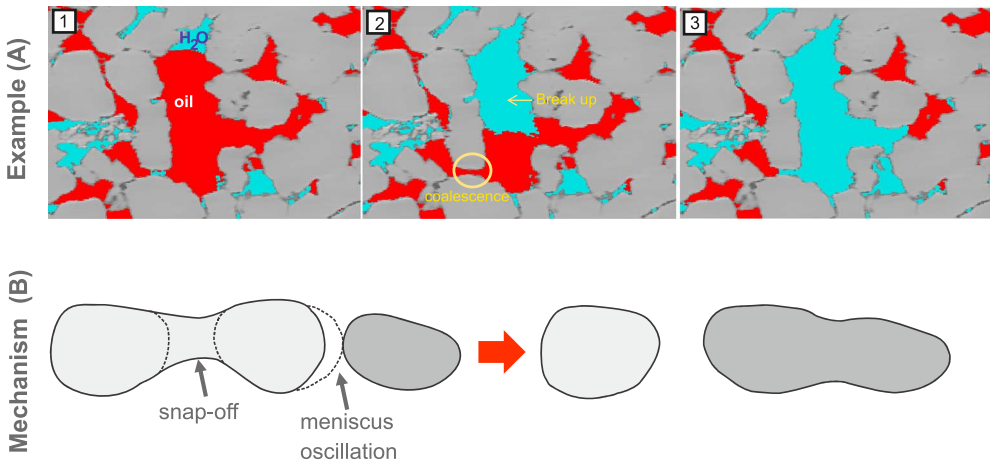

Figure 4. Internal redistribution of oil due to water-filling events leads to oil-filling events and coalescence between clusters in systems dominated by capillary forces as shown in tomography images of example (A) and sketched in (B).

At a frame rate of 40 s, our μCT imbibition experiment lacks the millisecond time resolution of the micromodel studies and, hence, cannot image the meniscus oscillation itself. However, the time resolution of the experiment is sufficient to image initial and final states of individual pore-scale displacement events (which occur once every few seconds in a larger sample [*DiCarlo et al.,* 2003; *Berg et al.,* 2013] with thousands of pores, i.e., the frequency in individual pores becomes comparable or even smaller than the frame rate in the experiment of 40 s), which allows us to identify correlated meniscus advancement, as shown in Figure 4. That provides further supporting evidence (a further example is shown in Figure S7) that snap-off events can trigger coalescence between two clusters that are in close proximity. In this way, isolated clusters can become reconnected.

4. Summary and Conclusions

Imbibition in porous rock is a two-stage process that involves a combination of connected pathway flow and ganglion dynamics as observed with fast μCT. Initially, wetting film swelling and subsequent local snap off of the nonwetting phase decreases the connectivity of the oil phase until it fragments into individual clusters. This breakup regime comprises multiple snap-off events which each causes displacement events larger than single pores. The associated meniscus oscillations in the connected oil-water interface elsewhere then, in turn, trigger coalescence events. The resulting ganglion dynamics caused by this coupled sequence of breakup and coalescence mobilizes oil clusters even though viscous forces from the average flow field are insufficient for their mobilization, i.e., the macroscopic or cluster-based capillary number $Ca^{\text{macro}} << 1$. This is a very prominent process, which underlines that average flow fields or externally applied injection rates and the associated capillary numbers have very little significance for pore-scale displacement processes. In immiscible displacement, the pore-scale dynamics are very fast [*Armstrong and Berg*, 2013], which leads to much higher local capillary numbers than the average flow field suggests and ultimately gives rise to a more complex set of nonlocal and cooperative effects ("ganglion dynamics"). The significance of such a ganglion dynamics process is that it contributes to the net transport of oil in addition to connected pathway flow over a wider oil saturation range, from about 75% (onset of ganglion dynamics) to as low as 30% where oil clusters become finally immobile. These findings should not only be considered for describing imbibition and related processes by numerical models (i.e., render quasi-static approaches as insufficient) [*Ferrari and Lunati*, 2014; *Raeini et al.,* 2014; *Moebius and Or*, 2014a], but more importantly ganglion dynamics that occurs at the cluster scale (i.e., clusters and their interactions) is a significant process regime bridging the pore and Darcy scale, which has been largely dismissed so far in most upscaling attempts.

Acknowledgments
Ab Coorn is acknowledged for the preparation of the rock samples. We would like to acknowledge Sarah Irvine and Marco Stampanoni (TOMCAT beamline at the Swiss Light Source (SLS), Paul Scherrer Institute (PSI)). We also thank Tom van Beusekom for recording the meniscus oscillations in the 2-D micromodel experiment. We gratefully acknowledge Shell for permission to publish this work. Supporting data are included as one test and seven figures; any additional data may be obtained from S.B. (email: steffen.berg@shell.com).

The Editor thanks Christian Huber and one anonymous reviewer for their assistance in evaluating this paper.

References

Andrew, M., B. Bijeljic, and M. J. Blunt (2013), Pore-scale imaging of geological carbon dioxide storage under in situ conditions, *Geophys. Res. Lett.*, *40*, 3915–3918, doi:10.1002/grl.50771.

Andrew, M., B. Bijeljic, and M. J. Blunt (2014), Pore-by-pore capillary pressure measurements using X-ray microtomography at reservoir conditions: Curvature, snap-off, and remobilization of residual CO_2, *Water Resour. Res.*, *50*, 8760–8774, doi:10.1002/2014WR015970.

Armstrong, R. T., and S. Berg (2013), Interfacial velocities and capillary pressure gradients during Haines jumps, *Phys. Rev. E*, *88*, 043010.

Armstrong, R. T., A. Georgiades, H. Ott, D. Klemin, and S. Berg (2014), Critical capillary number: Desaturation studies with fast X-ray computed microtomography, *Geophys. Res. Lett.*, *41*, 55–60, doi:10.1002/2013GL058075.
Armstrong, R. T., N. Evseev, D. Koroteev, and S. Berg (2015), Modeling the velocity field during Haines jumps in porous media, *Adv. Water Resour.*, *77*, 57–68.
Avraam, D. G., and A. C. Payatakes (1995), Flow regimes and relative permeabilities during steady-state two-phase flow in porous media, *J. Fluid Mech.*, *293*, 207–236.
Berg, S., H. Ott, A. Klapp, A. Schwing, R. Neiteler, N. Brussee, S. Irvine, and M. Stampanoni (2013), Real-time 3D imaging of Haines jumps in porous media flow, *Proc. Natl. Acad. Sci. U.S.A.*, *110*(10), 3755–3759.
Berg, S., et al. (2015), Onset of oil mobilization and non-wetting phase cluster size distribution, *Petrophysics*, *56*(1), 15–22.
Buckley, S., and M. Leverett (1942), Mechanism of fluid displacement in sands, *Trans. AIME*, *146*(01), 107–116.
Cense, A., and S. Berg (2009), The viscous-capillary paradox in 2-phase flow in porous media, paper SCA2009-13 presented at 23rd Annual Technical Symposium, Society of Core Analysts Noordwijk aan Zee, Netherlands.
Chaudhary, K., M. B. Cardenas, W. W. Wolfe, J. A. Maisano, R. A. Ketcham, and P. C. Bennett (2013), Pore-scale trapping of supercritical CO_2 and the role of grain wettability and shape, *Geophys. Res. Lett.*, *40*, 3878–3882, doi:10.1002/grl.50658.
Datta, S., J.-B. Dupin, and D. Weitz (2014), Fluid breakup during simultaneous two-phase flow through a three-dimensional porous medium, *Phys. Fluids*, *26*, 062004.
Deng, W., M. B. Cardenas, and P. C. Bennett (2014), Extended Roof snap-off for a continuous nonwetting fluid and an example case for supercritical CO_2, *Adv. Water Resour.*, *64*, 34–46, doi:10.1016/j.advwatres.2013.12.001.
Dias, M. M., and D. Wilkinson (1986), Percolation with trapping, *J. Phys. A*, *19*, 3131.
DiCarlo, D. A., J. I. G. Cidoncha, and C. Hickey (2003), Acoustic measurements of pore scale displacements, *Geophys. Res. Lett.*, *30*(17), 1901, doi:10.1029/2003GL017811.
Doster, F., and R. Hilfer (2011), Generalized Buckley-Leverett theory for two-phase flow in porous media, *New J. Phys.*, *13*, 123030.
Ferrari, A., and I. Lunati (2014), Inertial effects during irreversible meniscus reconfiguration in angular pores, *Adv. Water Resour.*, *74*, 1–13.
Herring, A., E. Harper, A. Andersson, A. Sheppard, B. Bay, and D. Wildenschild (2013), Effect of fluid topology on residual nonwetting phase trapping: Implications for geologic CO_2 sequestration, *Adv. Water Resour.*, *62*, 47–58.
Herring, A., L. Andersson, S. Schlüter, A. Sheppard, and D. Wildenschild (2015), Efficiently engineering pore-scale processes: The role of force dominance and topology during nonwetting phase trapping in porous media, *Adv. Water Resour.*, *79*, 91–102.
Hilfer, R. (1998), Macroscopic equations of motion for two-phase flow in porous media, *Phys. Rev. E: Stat. Nonlinear Soft Matter Phys.*, *58*(2), 2090–2096.
Hilfer, R. (2006a), Macroscopic capillarity and hysteresis for flow in porous media, *Phys. Rev. E: Stat. Nonlinear Soft Matter Phys.*, *73*, 016307.
Hilfer, R. (2006b), Macroscopic capillarity without a constitutive capillary pressure function, *Physica A*, *371*, 209–225.
Hilfer, R., and P. E. Øren (1996), Dimensional analysis of pore scale and field scale immiscible displacement, *Transp. Porous Media*, *22*(1), 53–72.
Iglauer, S., A. Paluszny, M. Blunt, and M. Blunt (2011), Residual CO_2 imaged with X-ray micro-tomography, *Geophys. Res. Lett.*, *38*, L21403, doi:10.1029/2011GL049680.
Joekar-Niasar, V., F. Doster, R. T. Armstrong, D. Wildenschild, and M. A. Celia (2013), Trapping and hysteresis in two-phase flow in porous media: A pore-network study, *Water Resour. Res.*, *49*, 4244–4256, doi:10.1002/wrcr.20313.
Krummel, A., S. Datta, S. Muenste, and D. Weitz (2013), Visualizing multiphase flow and trapped fluid configurations in a model three-dimensional porous medium, *AIChE J.*, *59*(3), 1022–1029.
Lake, W. L. (1989), *Enhanced Oil Recovery*, Prentice-Hall, N. J.
Lenormand, R., C. Zarcone, and S. Sarr (1983), Mechanism of the displacement of one fluid by another in a network of capillary ducts, *J. Fluid Mech.*, *135*, 337.
Moebius, F., and D. Or (2014a), Inertial forces affect fluid front displacement dynamics in a pore-throat network model, *Phys. Rev. E*, *90*(2), 023019.
Moebius, F., and D. Or (2014b), Pore scale dynamics underlying the motion of drainage fronts in porous media, *Water Resour. Res.*, *50*, 8441–8457, doi:10.1002/2014WR015916.
Mohanty, K., H. T. Davis, and L. E. Scriven (1987), Physics of oil entrapment, Society of Petroleum Engineers.
Murison, J., B. Semin, J.-C. Baret, S. Herminghaus, M. Schroeter, and M. Brinkmann (2014), Wetting heterogeneities in porous media control flow dissipation, *Phys. Rev. Appl.*, *2*, 034002.
Pak, T., I. B. Butler, S. Geiger, M. I. J. van Dijke, and K. S. Sorbie (2015), Droplet fragmentation: 3D imaging of a previously unidentified pore-scale process during multiphase flow in porous media, *Proc. Natl. Acad. Sci. U.S.A.*, *112*(7), 1947–1952.
Quéré, D. (1997), Inertial capillarity, *Europhys. Lett.*, *39*(5), 533–538.
Quéré, D., and É. Raphaël (1999), Rebounds in a capillary tube, *Langmuir*, *15*, 3679–33,682.
Raeini, A. Q., M. J. Blunt, and B. Bijeljic (2014), Direct simulations of two-phase flow on micro-CT images of porous media and upscaling of pore-scale forces, *Adv. Water Resour.*, *74*, 116–126.
Roof, J. G. (1970), Snap-off of oil droplets in water-wet pores, Society of Petroleum Engineers.
Schlüter, S., A. Sheppart, K. Brown, and D. Wildenschild (2014), Image processing of multiphase images obtained via X-ray microtomography: A review, *Water Resour. Res.*, *50*, 3615–3639, doi:10.1002/2014WR015256.
Youssef, S., E. Rosenberg, H. Deschamps, R. Oughanem, E. Maire, and R. Mokso (2014), Oil ganglia dynamics in natural porous media during surfactant flooding captured by ultra-fast X-ray microtomography, paper SCA2014-023 presented at International Symposium of the Society of Core Analysts held in Avignon, France, 11–18 Sept.